

Evaluation of Solar Radiation and Increase of the Productivity of a Photovoltaic Panel in Casablanca

Hind Ennasri¹, Asmaa Drighil², Rahma Adhiri³, Ahmed Fahli⁴, Mohamed Moussetad⁵

^{1-3,5}Laboratory of Engineering and Materials, Faculty of Sciences of Ben M'sik, Hassan II University
Boulevard CdtDriss El Harti, Casablanca, B.P.-7955, Morocco.

⁴Hassan I University, IbnouLhaytham Street, Settat, B.P.-577, Morocco.

Abstract

This article proposes the simulation of incident solar radiation on a horizontal and inclined plane in the city of Casablanca, then presents the results on a new minimum concentration system for photovoltaic module, sound geometric modeling and optimal work parameters. The low concentration system consists of a PV module and two mirrors, one on the left and symmetrically on the right along the PV module. Our goal is to maximize the direct radiation received from the PV, and the end of the article study is under the same meteorological conditions and the influence of a solar tracker on a photovoltaic panel.

Keywords: Radiation, Photovoltaic Panel, Low Concentration, Solar tracker.

I. INTRODUCTION

Combating green house effect gas emissions and protecting the environment make it urgent to control energy sources consumption and diversification: the use and development of renewable energy is the main solution [1]. A source of energy is said to be renewable if it is renewed rapidly enough to be considered inexhaustible at the human time scale. Among these sources, the most known and most profitable in the world is certainly solar energy, which is itself made up of different technological pathways [2]. Morocco has considerable solar potential. With 3000 hours of sunshine per year and an average irradiation of more than 5 KWh/m². The country intends to use this clean and inexhaustible energy massively in the coming years [3]. The knowledge of solar radiation, or solar radiation, on the surface of the Earth is of great interest in many fields. Climate science requires reliable and sufficient solar data to understand climate change[4]. Solar radiation data are often needed. However, the design and design of solar energy systems, such as solar water heaters, photovoltaic cells or thermal solar concentrators, requires data on solar radiation sufficiently precise to simulate, design, manage and optimize the productivity of these systems [5]. Photovoltaic conversion is the only way to directly transform energy through the sun as light into electricity. This transformation is carried out using photovoltaic cells still called photobatteries using the properties of semiconductor materials. Sunlight is a necessary and effective ingredient. Photovoltaic panels work with maximum efficiency as the incident light is perpendicular to their cells. Therefore, the energy efficiency of these systems

depends on the degree of use and conversion of solar radiation[6].

There are two ways to maximize useful energy: using mechanical orientation systems (solar followers), or concentration systems. Solar followers are designed and built to optimize the power efficiency of PV modules by ensuring that they are inclined towards the sun at all times during the day. For The use of the concentration system in photovoltaic panels is one of the important parameters for improving their performance, solar reflectors added to the photovoltaic panel allow to increase the amount of solar radiation intensity on the surface, several types configuration of reflectors such as parabolic, flat, spherical, parabolic reflectors[7]. This document is designed to increase the efficiency of photovoltaic systems. The analysis of a solar energy conversion system is based on a solar radiation assessment. We therefore need to know some aspects of the properties of solar radiation, in our case we have carried out a horizontal and inclined modeling and simulation of the incident solar radiation for the city of Casablanca, then based on the calculation of solar radiation, a study we have discussed to increase the efficiency of photovoltaic systems by using solar concentrator elements, as well as the reduction of the expensive photovoltaic surface Through a low concentration photovoltaic panel (LCPV), by two reflective flat mirrors, and at the end our photovoltaic panel should follow the sun so that the rays of the sun fall perpendicular to its surface, maximize the capture of solar energy and thus obtain the maximum output power. Tracking systems using controlled mechanisms that maximize the direct normal radiation received on PV Panel by a solar follower.

II.GLOBAL SOLAR RADIATION ESTIMATION ON A HORIZONTAL AND TILTED PLANE IN CASABLANCA CITY, MOROCCO

The sun declination is the angular distance from the sun north or south to the earth's equator. The maximum and minimum declination angle values of the earth's orbit produce seasons. Declination ranges between 23.45° north and 23.45° south. The northern hemisphere is inclined 23.45° far away from the sun, sometimes around December 21st., which is the summer solstice for the southern hemisphere and the winter solstice for the northern hemisphere. In the northern hemisphere and through 21 June, starting from nearly June 21st., the southern hemisphere is positioned in a way that it is 23.45° away from

the sun; meanwhile, it is winter solstice in the northern hemisphere. During the fall and spring equinoxes, which begin on March 21st. and September 21st. respectively, the sun passes directly over the equator [8]. The declination, in degrees, for any given day may be approximately calculated by the following equation:

$$\delta = 23.45 \sin\left[360 \cdot \left(\frac{284 + N}{365}\right)\right] \quad (1)$$

N: is the day of the year.

Solar hour angle (ω) is the angular distance between the hour circle of the sun and the local's meridian. For an observer on earth, the sun appears to move around the earth by the rate of 360° in 24 h or 15° per hour. The hour angle is defined as zero at local solar noon, the later being the time of day when the sun's altitude angle is at its greatest. The hour angle decreases by 15° for each hour before local solar noon and increases by 15° for each hour after solar noon. In other words the hour angle is set as positive after solar noon and negative before solar noon. Therefore, the hour angle can be written as follows [9]:

$$\omega = 15(TSV - 12) \quad (2)$$

TSV: is real time solar (in hours).

The zenith angle O_z is defined as the angle between the vertical and the line to the sun, which is the angle of incidence of a beam radiation on a horizontal plan, it can be calculated as[3]:

$$\cos(O_z) = \cos(\delta) \cos(\phi) \cos(h) + \sin(\phi) \sin(\delta) \quad (3)$$

ϕ : Latitude.

The solar altitude angle h is the angle between the horizontal and the line to the sun that is the complement of the zenith angle. It can be expressed using the following equation:

$$\sin(h) = \cos(\delta) \cos(\phi) \cos(\omega) + \sin(\phi) \sin(\delta) \quad (4)$$

Solar incident angle is the angle between the surface's normal and the sun's rays. If the surface is facing the equator ($\gamma = 0$), It can be expressed using the following equation:

$$\cos(O) = \cos(\delta) \cos(\phi - \beta) \cos(\omega) + \sin(\phi - \beta) \sin(\delta) \quad (5)$$

β : The slope.

1) Global radiation modeling on the horizontal plane:

The total radiation refers to as global solar radiation. Global solar radiation G (W/m²) is the sum of direct and diffuse radiations [10]:

$$G = G_{dir} + G_{diff} \quad (6)$$

The beam radiation G_{dir} is defined as solar radiation that travels from the sun to the earth's surface without any scattering by the atmosphere. It can be expressed using the following equation [11]:

$$G_{dir} = I_{oext} \exp\left(-\frac{m_h T_L}{0.9m_h + 9.4}\right) \sin(h) \quad (7)$$

The extraterrestrial solar irradiance I_{oext} is calculated from the solar constant, and the day number as follows:

$$I_{oext} = 1367 \left(1 - \frac{\sin(\delta)}{11.7}\right) \quad (8)$$

Where m_h is the atmospheric optical distance, called air mass. It can be written as follows:

$$m_h = \frac{1 - 0.1Z}{\sin(h) + 0.15(h + 3.885)^{-1.253}} \quad (9)$$

Z : Altitude of the place in (Km).

T_L is the Link turbidity factor. It gives an evaluation of the atmospheric extinction by gaseous molecules and aerosols. Its average value is given by the following expression [12]:

$$T_L = 2.5 + 16\beta_A + 0.5 \ln(w) \quad (10)$$

β_A is the Angstrom coefficient and w is the height of condensable water.

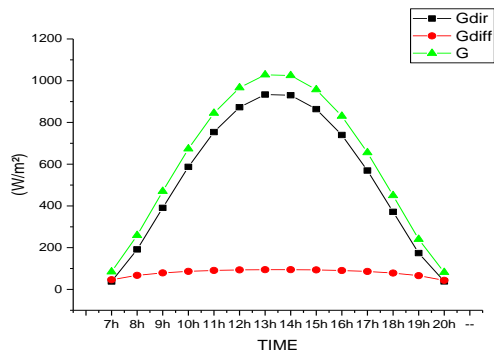
Table 1. β_A and w for different state of sky

state of the sky	β_A	w
pure sky	0.05	1
average sky	0.1	2
degraded sky	0.2	5

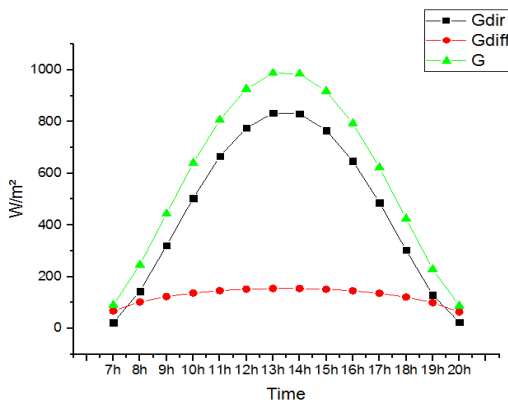
The diffuse radiation G_{diff} is solar reaching the earth's surface after having been scattered from the direct solar beam by molecules in the atmosphere. It can be expressed using the following equation:

$$G_{diff} = \frac{I_{oext}}{25} \sqrt{\sin(h)} [T_L - 0.5 - \sqrt{\sin(h)}] \quad (10)$$

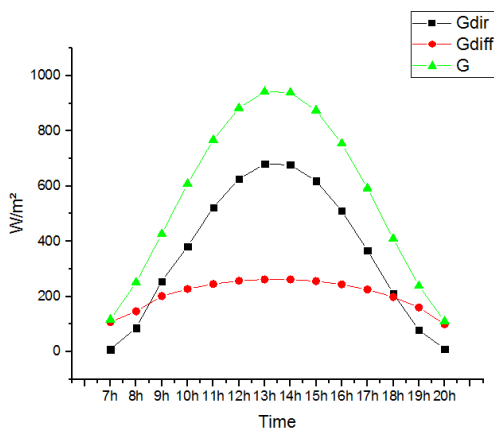
This work is related to the site of Casablanca, whose geographical coordinates are $L=7^\circ 36.6828'W$ for the Longitude, $L_o=33^\circ 35.2986'N$ for the latitude and $Z=27$ m for the altitude.



(a)



(b)



(c)

Fig. 1. Global solar radiation on a horizontal surface for June 21st. in Casablanca
 (a) pure sky ,(b) :average sky,(c) :degraded sky

Figures 1 (a,b,c) illustrate the three components of solar radiation for a pure, medium, and consecutively degraded sky for a horizontal plane in Casablanca, the global radiation G , which is the sum of the other two components, but the state of the sky has a great influence on direct and diffuse radiation. For a pure sky, direct radiation is the majority of the global radiation, whereas diffuse radiation is the But for a medium sky, direct radiation decreases, with the increase of diffuse radiation. Finally for a degraded sky, notice that diffuse radiation has continued to increase, and conversely to direct radiation that

has decreased, we find that the clearer the sky, the greater the overall radiation.

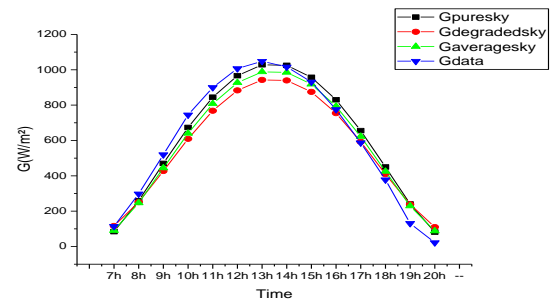


Fig. 2. Comparing weather data

Figure 2 shows a comparison between the results obtained by the simulation and the results of the measurements by the METEONORM meteorological data. In this figure, the practical measurements of the global incident radiation on a horizontal plane, as well as the calculated values for the three states of the sky are shown. For 21 June, the values calculated with a pure sky were the most suitable for the measurements. The confrontation of the numerical results obtained, together with the meteorological measurements, showed a satisfactory agreement on the condition of changing the state of the sky, with the change of seasons.

2) Solar radiation on tilted surface:

The hourly total irradiation incident on a tilted surface is composed of direct radiation, ground reflected radiation and sky-diffuse radiation components [13].

The direct radiation a surface receives depends on the angle of incidence of the solar rays.

The diffuse radiation received by the inclined surface does not depend on the orientation of the plane and does not come from the entirety of the sky vault or the ground nearby – it only comes from the part of the sky that the surface. Therefore, for the calculation of solar radiation on an inclined surface, a conversion factor should be taken into account for each of the components. The conversion factor for the direct solar irradiance R_b , is the ratio of the direct solar irradiance on the inclined surface, to that on a horizontal surface G_{dir} , is giving by:

$$R_b = \frac{\cos \theta}{\cos \theta_z} \quad (11)$$

The diffuse radiation is based on the assumption that the diffusion is isotropic, i.e. that it is uniformly received from the entire sky dome. The conversion factor for diffuse radiation R_d is the ratio of diffuse radiation incident on the inclined surface to that on the horizontal plane G_{diff} . The diffuse radiation coming from the celestial dome, only a percentage reaches the

inclined surface. This percentage is the ratio of the portion of celestial dome that the inclined surface, to the entire hemispherical surface of the celestial dome. In the isotropic model and for an unshaded inclined surface on the ground, with slope β , the conversion factor is the view factor to the sky and is given by:

$$R_d = \frac{1 + \cos \beta}{2} \quad (12)$$

The conversion factor for the reflected radiation R_r is the ratio of reflected radiation incident on the inclined surface to that on the horizontal. However, the reflected on the horizontal plane, is the product of the diffuse reflectance ρ of the surroundings and the total solar irradiance on the horizontal G . As in the previous case, assuming that the reflected irradiance is isotropic, then for an inclined surface tilted at slope β from the horizontal, the conversion factor is the view factor to the ground and is given by:

$$R_r = \frac{1 - \cos \beta}{2} \quad (13)$$

The total solar radiation on the tilted surface is the sum of three terms:

$$G_\beta = G_{dir} \cdot \frac{\cos \theta}{\cos \theta_z} + G_{diff} \cdot \frac{1 + \cos \beta}{2} + G_r \cdot \frac{1 - \cos \beta}{2} \quad (14)$$

The titled angle of the surface will be fixed for each day and is calculated by following equation:

$$\beta = |\phi - \delta| \quad (15)$$

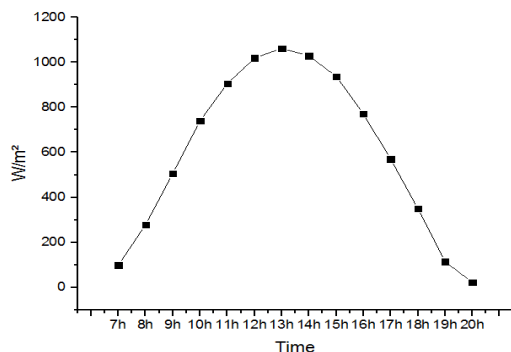


Fig.3. Global solar radiation on a titled surface for 21 June in Casablanca

In the northern hemisphere, the south facing orientation is considered the best for solar sensor. However, the angle of the panel remains to be determined for each given site. Figure 3 shows the variation in the daily global radiation received by a flat surface at the Casablanca site. The illumination typically varies as shown in Figure 3 during an undisturbed day (June 21), it increases as early as daybreak to a maximum value of 1062.42 W/m² at TSV=1 p.m., then decreases again until the night falls. In this case, we conclude that to capture the maximum amount of energy received from the sun, the south

facing plane must be positioned on what is called an optimal pitch range. For 21 June, Casablanca has a 10° angle of inclination.

III. SIMULATION OF PHOTOVOLTAIC MODULE

The four-parameter equivalent circuit is shown in Figure 4.

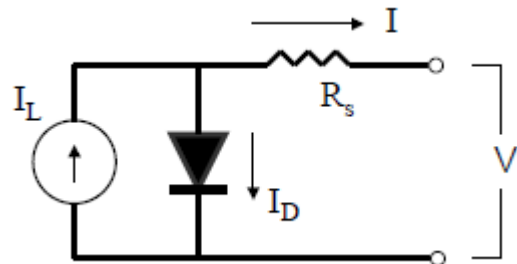


Fig.4. Equivalent electrical circuit in the 4-parameter model[14]

The IV characteristics of a PV change with both insolation and temperature. The PV model employs these environmental conditions along with the four module constants $I_{L,ref}$, $I_{0,ref}$, γ , and R_s to generate an IV curve at each time step. The current-voltage equation of circuit shown in Figure 4 is as follows:

$$I = I_L - I_0 \left[\exp\left(\frac{q}{\gamma k T_c} (V + IR_s)\right) - 1 \right] \quad (16)$$

q : Electron charge constant.

γ : Empirical PV curve-Fitting parameter.

k : Boltzmann constant [J/K].

T_c : Module temperature [K].

V : Voltage.

I : Current.

R_s : Module series resistance [Ω].

The photocurrent I_L depends linearly on incident radiation:

$$I_L = I_{L,ref} \frac{G}{G_{ref}} \quad (17)$$

$I_{L,ref}$: Module photocurrent at reference conditions.

G : Total radiation incident on PV array.

G_{ref} : Incident radiation at reference conditions.

The diode reverse saturation current I_0 is a temperature dependent quantity:

$$\frac{I_0}{I_{0,ref}} = \left(\frac{T_c}{T_{C,ref}} \right)^3 \quad (18)$$

$I_{0,ref}$: Diode reverse saturation current at reference conditions.

$T_{C,ref}$: Module Temperature at reference conditions [K].

Table 2. PV module parameters [15]

Parameters	Value
Area	1.62
Module efficiency	17.28%
Short-circuit current I_{sc}	9.03A
Open-circuit voltage V_{oc}	39.91V
Voltage at maximum power point U_{mpp}	31.43V
Current at maximum power point I_{mpp}	8.91A
Short-circuit current temperature coefficient	0.05%/°C
Open-circuit voltage temperature coefficient	-0.29%/°C
Number of cells in series N_s	60

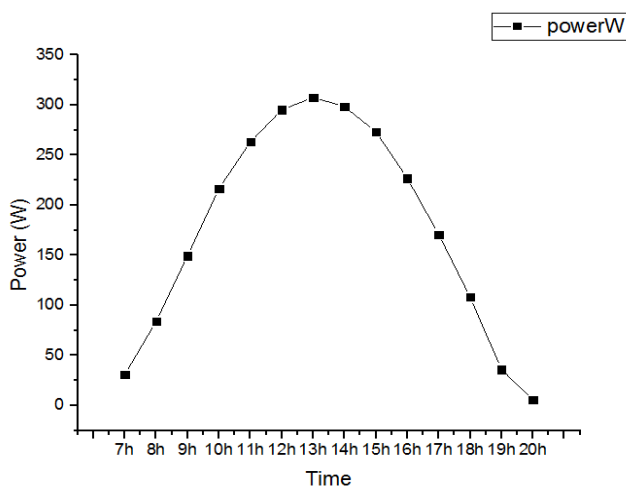


Fig.5. Electric power by product photovoltaic panel in Casablanca

Figure 5 shows the variation of the electric power produced by the photovoltaic panel, their characteristics are shown in Table 2, during the day of June 21, with an inclination of 10° , this variation is generally influenced by several parameters, but particularly by solar irradiation. The electrical power is maximum at 13.00. In order to increase the productivity of this panel two proposals are studied:

1. The use of solar concentrators.
2. The use of mechanical orientation systems called solar followers.

IV. PHOTOVOLTAIC PANEL WITH LOW CONCENTRATION:

The improvement of the performance of a photovoltaic system can be achieved by the increase in energy delivered by the field

of the photovoltaic modules of the system. This can be achieved by optimizing the inclination of the modules, depending on the season and the location of installation. The output of the photovoltaic generator can also be improved by increasing the incidence of solar radiation on the modules, with flat reflectors placed between the rows of the constituent modules of the photovoltaic generator. Different types of reflectors are attached to the side of the single PV module. This configuration has significantly improved the energy generated by the solar module. The geometrical model of the concentration system is attached in Figure 6. The solar array reflects by each mirror cover a half of the panel surface. Thus, the two lateral mirrors reflect the solar light on the entire surface of the PV panel [16-17].

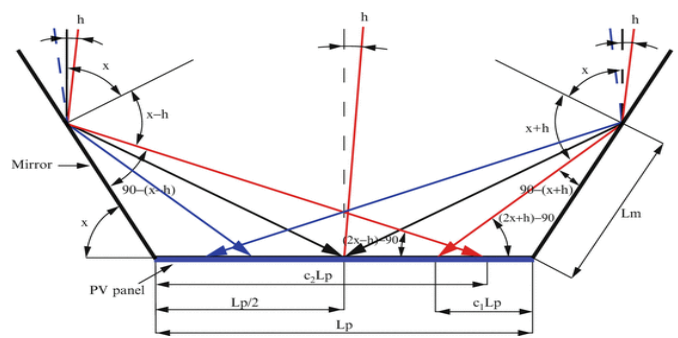


Fig.6. Geometric model of LCPV system

The global radiation received normally by the inclined plane provided with concentrator elements type lateral mirrors is described by the relation [18]:

$$(19) \quad G_{onc} = G_{\beta} + \sum G_{M_{1,2}}$$

Where $G_{M_{1,2}}$ is the irradiation reflected by the two mirrors:

$$(20) \quad = G_{dir} \cos(h_{R_{1,2}})$$

Where $h_{R_{1,2}}$ is the incidence angle formed between the ray reflected by each mirror and the normal to the photovoltaic panel.

$$\begin{aligned} \cos(h_R) &= \sin \delta (\sin \phi \cos x - \cos \phi \sin x \cos \gamma) \\ &+ \cos \delta \cos \omega (\cos \phi \cos x + \sin \phi \sin x \cos \gamma) \\ &+ \cos \delta \sin x \sin \gamma \sin \omega \end{aligned} \quad (21)$$

In our case our goal is to reduce the surface of the mirror, thus to reduce the overall size of the system, by stating that the solar radiation falling from each mirror sweeps about half of the PV surface. In this case we start with knowing the length of the PV,

L_p ; considering that the solar ray covers $L_p/2$, we determine the value of L_m , length of the mirror. The ratio between L_p and L_m was calculated:

$$(22) \frac{L_m}{L_p} = \frac{-\cos(2x)}{\cos(x)}$$

The geometrical parameters that had been taken into consideration for simulation are presented below: $\beta=10^\circ$; $x = 53, 63^\circ$; $L_m=496\text{mm}$; $L_p=992\text{mm}$;

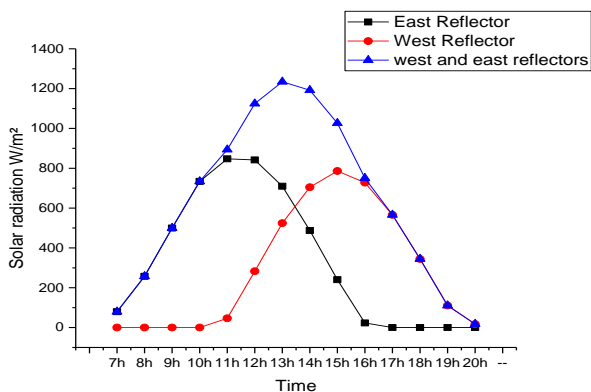


Fig.7. The solar radiation reflected by each mirror

Figure 7 shows the variation of solar radiation reflected by the two reflectors East and West on the photovoltaic panel, in the morning the Reflector East reflects more solar radiation on the photovoltaic panel, and in the afternoon the Reflector West reflects more radiation, so both reflectors work alternately. The sum of the two solar radiations reflected on the photovoltaic panel results in a parabolic shape curve, identical in shape to that of the global solar radiation received directly on the photovoltaic panel.

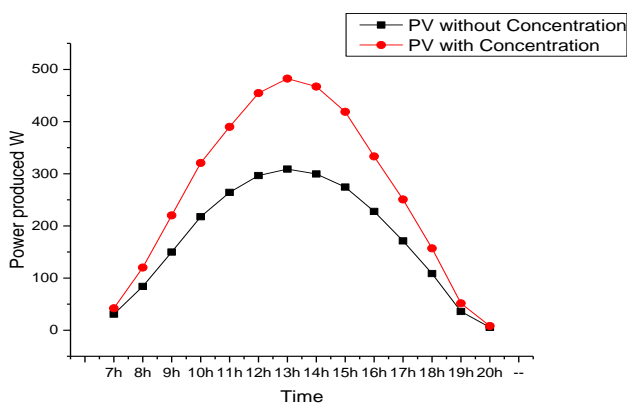


Fig.8. Electric power by product photovoltaic panel with low concentration in Casablanca

Therefore, the graphic evolution of electrical power produced by the photovoltaic panel with a concentration system, for the same conditions as previously, is shown in Figure 8. The graph notes that reflectors have a significant influence on the electrical power produced. For the simulation performed, the optimal angle value is 53° . The solar radiation absorbed by an

LCPV panel depends on the geometric parameters, the orientation of the photovoltaic panel, and the season.

V. PHOTOVOLTAIC PANEL WITH SOLAR TRACKER:

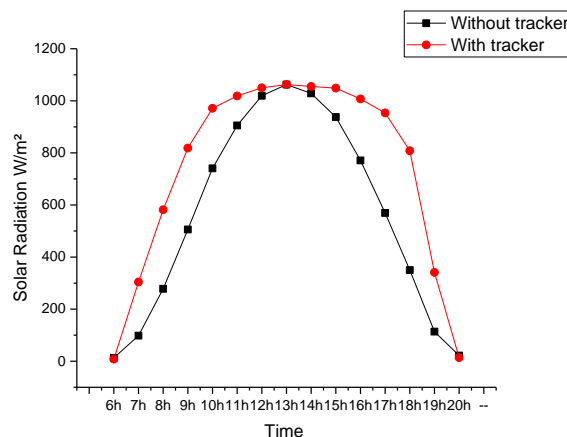


Fig.9. Solar irradiation for a photovoltaic panel with solar tracker.

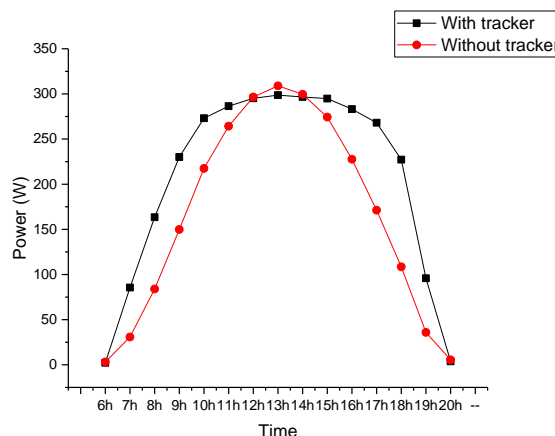


Fig.10. Electrical power produced by a photovoltaic panel with solar tracker.

One method of optimizing available solar energy conversion with real implementation possibilities is the use of tracking systems. Literature shows that the uses of tracking systems go from 20% to 40% of the amount of energy produced by conversion [9]. In practice, there are two types of tracking systems: One-axis and two axis tracking systems, Depending on the apparent displacement of the sun on its trajectory, the monitoring phase consists of increasing or decreasing the azimuth and/or elevation of the solar panel.

Figure9 shows the solar radiation received on the photovoltaic panel system. As can be seen in this figure, the two-axis solar follower system is more efficient.

Figure 10 illustrates the power supplied by the photovoltaic panel on the follower in relation to that placed with a fixed inclination. The results show that the power supplied by the

panel on the follower is greater than that supplied by the panel with a fixed inclination and orientation towards the south with an angle of inclination of 10° .

The curves also show that the value of the solar energy collected by the panel with a fixed inclination and a south orientation is similar to that obtained with the panel placed on the solar follower between 11.00 and 14.00, when the sun passes through the Zenith. However, it moves away during sunrise and late afternoon hours.

V.CONCLUSION

This work presents the estimation of solar radiation on a horizontal plane as well as an inclined plane in the city of Casablanca. The measurements collected by the meteorological stations validate the model chosen for the prediction and the estimation of simulations. According to the two proposals to study for the improvement of the productivity of the photovoltaic panel we have noticed that the two proposals have a positive impact, for the photovoltaic panel at low concentration increases the productivity of the photovoltaic panel with a percentage of 45%, and relative to the solar tracker the improvement is significant but less than the solar concentrator.

REFERENCES

- [1] Samuel Asumadu Sarkodie, Vladimir Strezov. Effect of foreign direct investments, economic development and energy consumption on greenhouse gas emissions in developing countries; *Science of the Total Environment* 646 (2019) 862–871.
- [2] VV Quaschnig, book of Renewable energy and climate change.
- [3] Chambre Française de Commerce et d'Industrie du Maroc (CFCIM). *L'énergie solaire au Maroc*.
- [4] N. B. Xiang. Revisiting the Question: The Cause of the Solar Cycle Variation of Total Solar Irradiance; *Advances in Astronomy* Volume 2019, Article ID 3641204, 9 pages.
- [5] Antonio Gaglianoa, Giuseppe M. Tinaa, Francesco Noceraa, Alfio Dario Grassoa, Stefano Anelia. Description and performance analysis of a flexible Photovoltaic/Thermal (PV/T) solar system. *Renewable Energy* (2018), doi: 10.1016/j.renene.2018.04.057.
- [6] Fabian Benavente, Anders Lundblad, Pietro Elia Campana, Yang Zhang, Saúl Cabrera, Göran Lindbergh. Photovoltaic/battery system sizing for rural electrification in Bolivia: Considering the suppressed demand effect, *Applied Energy* Volume 235, 1 February 2019, Pages 519-528.
- [7] A. Luque, V.M. Andreev, *Concentrator Photovoltaics*, Springer-Verlag, Berlin Heidelberg, 2007.
- [8] Iqbal, M. *An Introduction to Solar Radiation*; Academic Press: Toronto, ON, Canada, 1983.
- [9] T. Maatallah, S. El Alimi, S. Ben Nassrallah, Performance modeling and investigation of fixed, single and dual-axis tracking photovoltaic panel in Monastir city, Tunisia, *Renewable and Sustainable Energy Reviews*, Vol. 15, Issue 8, (2011), pp. 4053-4066.
- [10] DOSTAL, Z. and M. DULIK. Vykon slnecneho ziarenia na povrchu Zeme. In: *Proceedings of RESpect. Poracska Dolina: Faculty of Electrical Engineering (University of Zilina)*, 2013, pp. 47–65. ISBN 978-80-553-1405-1.
- [11] B. Ould Bilal, V. Sambou, C.M.F. Kebe, M. Ndongo, P.A Ndiaye, Etude et modélisation du potentiel du site de Nouakchott et de Dakar, *Journal des Sciences*, Vol. 7, N°4, (2007), pp. 57-66.
- [12] Mohamed ansoumane camara modélisation du stockage de l'énergie photovoltaïque par super-condensateurs, thèse de doctorat, Université Paris-Est Creteil. (2011).
- [13] Ali Mohammad Noorian, Isaac Moradi, Gholam Ali Kamali, Evaluation of 12 models to estimate hourly diffuse irradiation on inclined surfaces *Renewable Energy* 33 (2008) 1406–1412
- [14] R. Khezzer , M. Zereg , A. Khezzer. Modeling improvement of the four parameter model for photovoltaic modules, *Solar Energy* 110 (2014) 452–462
- [15] Photovoltaic modules. Available: www.eurenergroupp.com
- [16] Alboteanu, I.L.; Ravigan, F.; Degeratu, S.; Sulea, C. Aspects of designing the tracking systems for photovoltaic panels with low concentration of solar radiation. In *Computational Problems in Engineering II*; Springer-Verlag: Cham, Switzerland, 2014.
- [17] Alboteanu, I.L.; Bulucea, C.A.; Degeratu, S. Modeling of solar irradiation absorbed by a photovoltaic panel with low concentration. In *Recent Advances in Environmental Sciences and Financial Development, Proceedings of the 2nd International Conferences on Environment, Energy, Ecosystems and Development—EEEAD 2014*, Athens, Greece, 28–30 November 2014; pp. 16–21.
- [18] Hermenean, I.; Vişa, I.; Duţă, A.; Diaconescu, D. Modeling and Optimization of a CPV System with Equatorial Tracking. *Bull. Transilv. Univ. Braşov. Ser. I Eng. Sci.* 2010, 3, 79–86.